

Discovery of Inhibitors of Four Bromodomains by Fragment-Anchored Ligand Docking

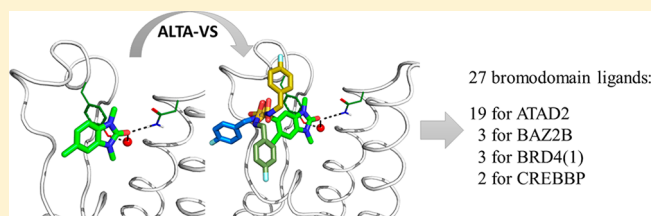
Jean-Rémy Marchand,[†] Andrea Dalle Vedove,[‡] Graziano Lolli,[‡] and Amedeo Caflisch^{*,†}

[†]Department of Biochemistry, University of Zürich, CH-8057, Zürich, Switzerland

[‡]Centre for Integrative Biology, University of Trento, I-38123, Povo, Italy

S Supporting Information

ABSTRACT: The high-throughput docking protocol called ALTA-VS (anchor-based library tailoring approach for virtual screening) was developed in 2005 for the efficient *in silico* screening of large libraries of compounds by preselection of only those molecules that have optimal fragments (anchors) for the protein target. Here we present an updated version of ALTA-VS with a broader range of potential applications. The evaluation of binding energy makes use of a classical force field with implicit solvent in the continuum dielectric approximation. In about 2 days per protein target on a 96-core compute cluster (equipped with Xeon E3-1280 quad core processors at 2.5 GHz), the screening of a library of nearly 77 000 diverse molecules with the updated ALTA-VS protocol has resulted in the identification of 19, 3, 3, and 2 μ M inhibitors of the human bromodomains ATAD2, BAZ2B, BRD4(1), and CREBBP, respectively. The success ratio (i.e., number of actives in a competition binding assay *in vitro* divided by the number of compounds tested) ranges from 8% to 13% in dose–response measurements. The poses predicted by fragment-based docking for the three ligands of the BAZ2B bromodomain were confirmed by protein X-ray crystallography.



INTRODUCTION

In vitro fragment-based drug design is an attractive strategy to cover the chemical space of binders at a reduced cost and a more efficient approach than brute force high-throughput screens.¹ On the computational side, high-throughput docking is a valuable asset when it comes to finding small molecule binders of proteins.^{2,3} It can enrich screening libraries usually with 1% to 10% hit rates.^{4,5} Recently, evidence has accumulated on the success of fragment–hit identification with force field-based approaches which make use of explicit⁶ or implicit^{7–9} solvent treatment.

In 2005, an efficient computational approach that combines the advantages of high-throughput docking with those of fragment-based hit identification was introduced.^{10,11} The computational protocol was later called anchor-based library tailoring approach virtual screening (ALTA-VS, Figure 1).¹² ALTA-VS is a four-step protocol: (1) decomposition of the chemical library into its essential rigid fragments; (2) docking of the fragments and evaluation of binding energy (with generalized Born approximation of electrostatic solvation effects); (3) flexible docking of the parent molecules that contain the top ranking fragments which are used as noncovalent binding anchors during docking (three anchor fragments for each parent molecule in the original version of ALTA-VS); and (4) energy minimization with final evaluation of binding energy including desolvation effects in the continuum dielectric approximation (finite-difference Poisson equation). An essential element of the ALTA-VS approach is the much higher efficiency of the fragment-anchored docking of

a set of 10^3 to 10^4 parent molecules than the docking of a multimillion compound library and, importantly, the high accuracy of docked poses of fragments.^{5,7–9} The successful identification of hit compounds by the ALTA-VS approach has been reported for several protein targets.^{10–14}

Here we report on an updated version of the ALTA-VS method, which has three improvements with respect to the original protocol.^{10,11} First, a single anchor fragment is required for flexible ligand docking instead of three fragments as in the original version of ALTA-VS. Second, it employs an energy function without any fitting parameters. These two improvements result in a broader range of applicability, in particular to protein targets with a small binding site and/or for which inhibitors have not been disclosed. Third, we make use of a transferable force field which treats in a consistent way the parameters of proteins (CHARMM36)¹⁵ and organic compounds (CGenFF).^{16,17}

Bromodomains are left-handed four-helix bundles of about 110 residues.¹⁸ The 61 human bromodomains, found in 46 proteins, bind acetylated peptides and in particular acetylated histone tails.¹⁹ The bromodomain binding pocket has been heavily investigated, both in complex with physiological ligands or with synthetic small molecules.²⁰ The binding pocket of the natural ligand (acetylated lysine in histone tails and other proteins) is formed on one of the two ends of the four-helix bromodomain fold by the loop connecting the helix αZ and αA ,⁷⁶

Received: June 6, 2017

Published: September 1, 2017

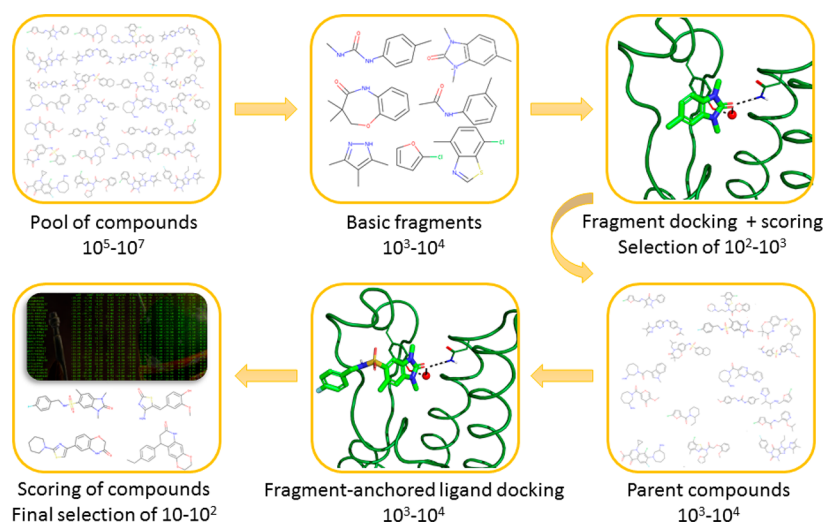


Figure 1. Anchor-based library tailoring approach for virtual screening (ALTA-VS). A chemical library, with up to tens of millions of compounds, is decomposed in nonrotatable fragments, which are docked and scored. Parent compounds containing the top ranking fragments are retrieved and docked with tethering of the fragment headgroup. Those docked molecules are then further energy minimized with a force field and evaluation of electrostatic desolvation effects by the finite-difference Poisson approach. Thus, the ALTA-VS protocol selects $10\text{--}10^2$ compounds for in vitro validation (bottom, left panel) from libraries of $10^5\text{--}10^7$ molecules (top, left) by docking only $10^3\text{--}10^4$ fragments (top, middle) and $10^3\text{--}10^4$ compounds (bottom, middle).

77 called ZA loop, and the loop linking the α B and α C helices,
78 named the BC loop. The bromodomain family has high
79 therapeutic interest, with 14 inhibitors currently in clinical
80 trials.^{21,22} Their crucial implication in epigenetics affects gene
81 expression with potential involvement in cancer, inflammation,
82 and neurological diseases.²³

83 The new version of ALTA-VS is applied here to screen a
84 library of nearly 77 000 compounds for the bromodomains of
85 ATAD2, BAZ2A, BAZ2B, BRD4(1), and CREBBP. In contrast
86 to previous in silico screening campaigns which focused each
87 on a single protein target and made use of different
88 libraries,^{5,24,25} the same protocol (updated ALTA-VS) and
89 library were employed in the present study for five related
90 proteins. The updated ALTA-VS protocol has led to the
91 discovery of 27 small-molecule inhibitors with micromolar
92 potency for the target bromodomain and, in particular, 15
93 compounds with an affinity below $100\ \mu\text{M}$. Furthermore, the
94 predicted binding mode of the three inhibitors of the BAZ2B
95 bromodomain was confirmed by protein X-ray crystallography.

96 ■ THEORY

97 The ALTA-VS strategy consists of four steps here illustrated in
98 detail. The first step is the decomposition of each molecule of
99 the library into rigid fragments, which are defined such that all
100 rotatable bonds are cut. The original library is usually a
101 collection of commercially available compounds. In contrast,
102 the generated fragment library includes molecules that may not
103 be synthesizable, which is not a limitation as the final ranking
104 and selection for experimental validation are done for the
105 original compounds (Figure 1).

106 In the second step, the fragment library is docked with the
107 program SEED^{26,27} which requires about one second per
108 fragment.⁵ SEED docks the rigid fragments in the target
109 binding pocket by an exhaustive search with intermolecular
110 hydrogen bond distances as restraints. For each fragment
111 position and orientation the binding energy is evaluated with a
112 force field and the generalized Born implicit solvation model is

used to approximate the electrostatic contribution to the
binding free energy.²⁸

For the third step, the fragments with the most favorable
calculated binding energy are selected. Their parent com-
pounds are retrieved and docked with a flexible docking tool.
Here we used RDock,²⁹ which is adequate for the ALTA-VS
approach as it can dock compounds with a tethered
substructure. For each parent compound, the substructure
corresponding to the docked fragment is tethered in the
binding pocket and the orientation of the rest of the molecule is
optimized by a search in the space of rotatable bonds. Flexible
docking software usually employ a very crude approximation of
the binding free energy, especially for the solvation and
torsional energies. Those approximations can lead to
implausible binding poses, which result in a large amount of
false positives in the top ranked compounds. Moreover,
previous reports have emphasized the difficulties in docking
highly flexible compounds.³⁰ In the ALTA-VS approach the size
of the conformational space of flexible ligands is reduced
substantially by fragment anchoring. The original implementa-
tion of the ALTA-VS procedure¹² made use of the SEED
docking of fragments in three different subpockets and
subsequent linkage of the fragments with a flexible docking
algorithm developed in-house called FFLD.³¹ This approach
required the empirical definition of three subpockets, which
might not be possible for targets with small and/or shallow
binding site. For instance, one can hardly define three
subpockets in the binding site of bromodomains.³² The
availability of open source software for flexible docking with
possibilities of substructure tethering such as RDock gave us
the opportunity to sample docking positions of putative ligands
with a single anchored headgroup.

Once the molecules are docked, the fourth and last step
consists in minimizing the energy of the poses and rescored
them, i.e., estimating their binding free energy. Here, we
employ the Poisson equation solver³³ of the CHARMM
package³⁴ to compute the electrostatic component of the
binding process, including solvation energy, and add the 150

151 electrostatic term to the ligand/bromodomain van der Waals
152 energy. Importantly, a force field-based energy function was
153 used here without any fitting parameters, while the original
154 ALTA-VS protocol used a scoring function based on a linear
155 interaction energy model with two multiplicative parameters for
156 van der Waals and electrostatics contributions, respectively.¹²

157 ■ EXPERIMENTAL SECTION

158 **Assembly of the Screening Library.** The chemical
159 library³⁵ of the Lausanne Bioscreening Facility was used here
160 because it is a large collection of diverse compounds which are
161 commercially available. The library we assembled from their
162 service contained 76 731 chemically diverse molecules from
163 seven vendors (see [Supporting Information](#), section S1).

164 We used the ChemAxon software suite to prepare the library,
165 with a special focus on protonation and tautomeric states. To
166 the best of our knowledge and at the time of the study, the
167 ChemAxon software suite relied on the largest training set for
168 organic molecule pK_A calculations.³⁶ The electronic library was
169 processed and cleaned with the Calculator Plugins of Marvin
170 15.1.5.0, 2015, ChemAxon (www.chemaxon.com) with the
171 following steps:

- 172 • ChemAxon structurechecker module to check for
173 aromaticity and valence issues.
- 174 • ChemAxon stereoisomers module to generate a max-
175 imum of four stereoisomers per molecule.
- 176 • ChemAxon dominanttautomerdistribution module to
177 generate tautomers (protomers) at pH 7.2, filtering out
178 structures with a predicted occupancy below 25%.
- 179 • ChemAxon leconformer module to generate one clean
180 conformer per molecule (optimization level 3, MMFF94,
181 in vacuo).

182 This preparation protocol generated 135 840 structures,
183 corresponding to 75 830 unique molecules. Thus, the loss of
184 molecules was about 1%. Chemical library properties, e.g.,
185 molecular weight, number of hydrogen bond donors, heavy
186 atom count, are available in the [Supporting Information](#),
187 section S1.

188 **Fragmentation of the Library.** The molecules were
189 fragmented into their essential rigid fragments by cutting all
190 rotatable bonds with a script relying on the RDKit.³⁷ Rotatable
191 bonds were defined according to the following SMARTS
192 pattern: `[!$([NH]!@C(=O))&!D1&$(*#*)]&!`
193 `@[$([NH]!@C(=O))&!D1&!$(*#*)]`. Missing valences
194 were filled with a hydrogen atom, which only for a small
195 number of fragments led to spurious hydrogen-bond donors.
196 The generated virtual fragments were subsequently unquified
197 with Open Babel,³⁸ which led to 6436 rigid fragments. In a next
198 step, we prepared the fragments for docking with SEED. The
199 software CGenFF 1.0 was used to assign CGenFF 3.0.1
200 parameters to the fragments.^{16,17} After parametrization and
201 preparation, 6406 fragments were left for docking, which
202 corresponds to a loss of only 0.5% of the fragments during the
203 parametrization.

204 **Preparation of Protein Targets.** Crystal structures of
205 proteins were selected with a preference for those solved in the
206 laboratory of the authors and according to the following
207 rationale: (1a) does an in-house holo crystal structure exist? Yes
208 for BAZ2B (PDB code 5e73), BRD4(1) (4pci), and CREBBP
209 (4tqn). (1b) If not, is there a holo crystal structure available in
210 the literature? Yes for ATAD2 (5a5r) and BAZ2A (4bqm). (2)
211 We chose the structure with the most potent small organic

binder at the time of the study (in-house for 1a and in the PDB
212 for 1b), with the exception of BAZ2A for which a single holo
213 structure was available bound to an acetylated histone tail
214 peptide. Hydrogen atoms of the protein and the six structurally
215 conserved water molecules¹⁹ were added and minimized with
216 CHARMM.³⁴ The minimization took place in the presence of
217 the ligand of the crystal structure. Heavy atoms were fixed,
218 while added atoms were free to move during a two-stage
219 minimization in vacuo which consisted of 5000 steps of steepest
220 descent and 100 000 steps of conjugate gradient with
221 convergence threshold based on the energy gradient of 0.01
222 kcal/(mol Å). The convergence threshold was reached in all
223 case. 224

Docking and Selection of Anchor Fragments. Docking
225 of fragments was carried with our in-house docking software
226 SEED^{26,27} with the same protocol for the five bromodomains.
227 The six conserved water molecules were considered part of the
228 receptor. The binding site was defined by two residues and two
229 structurally conserved water molecules. The two residues are
230 the evolutionary conserved asparagine whose side chain is
231 involved in a hydrogen bond with the acetyl group of the
232 natural ligand (Asn1064 for ATAD2, Asn1873 for BAZ2A,
233 Asn1944 for BAZ2B, Asn140 for BRD4(1), Asn1168 for
234 CREBBP), and the central residue of the so-called WPF shelf
235 (Val1008 for ATAD2 which has an RVF shelf, Pro1817 for
236 BAZ2A, Pro1888 for BAZ2B, Pro82 for BRD4(1), Pro1110 for
237 CREBBP). The two water molecules are the one that bridges
238 the acetyl group to the conserved tyrosine (Tyr1021 for
239 ATAD2, Tyr1830 for BAZ2A, Tyr1901 for BAZ2B, Tyr97 for
240 BRD4(1), Tyr1125 for CREBBP) and the conserved water
241 molecule the farthest from it (HOH3081 for ATAD2,
242 HOH2214 for BAZ2A, HOH2138 for BAZ2B, HOH381 for
243 BRD4(1), HOH1339 for CREBBP). The interior dielectric
244 constant of the protein was set to 2.0, and the solvent dielectric
245 constant, to 78.5. 246

Following previous evidence of the importance of key
247 hydrogen bonds as a filter,¹³ we discarded the fragments that
248 did not have any hydrogen bond-acceptor atom within a
249 distance of 4 Å from the side chain nitrogen of the conserved
250 asparagine. Three energy-based functions were used to filter
251 compounds from the different energy components calculated
252 by SEED: Delta electrostatics, total energy efficiency, and
253 electrostatic efficiency. The Delta electrostatics is the difference
254 between the fragment/receptor electrostatic interaction and the
255 electrostatic free energy of hydration of the fragment (both
256 calculated with the generalized Born approach). It measures the
257 intermolecular electrostatic interaction relative to the free
258 energy of solvation of the fragment assuming a rigid
259 conformation of both protein and fragment. The total energy
260 efficiency is the total binding free energy divided by the number
261 of non-hydrogen atoms (HAC = heavy atom count), which
262 tend to penalize large ligands. The electrostatic efficiency is the
263 fragment/receptor electrostatic interaction divided by HAC.
264 This term tends to favor compounds with favorable electro-
265 static interaction with the protein, normalized by the number of
266 heavy atoms to avoid a systematic bias toward large polar
267 compounds. 268

For each of the five bromodomains, the top 150 fragments
269 were selected individually based on Delta electrostatics, total
270 energy efficiency, and electrostatic efficiency. Then, the
271 fragment selections between targets were compared to be
272 mutually exclusive for each target. In other words, only
273 fragments selected for a single bromodomain were retained, i.e.,
274

Table 1. Statistics of the ALTA-VS Protocol in the Five Bromodomains

	ATAD2	BAZ2A	BAZ2B	BRD4(1)	CREBBP
number of fragments (out of 6406)	142	137	184	210	192
unique parent compounds	2954	894	2791	2520	2476
conformers generated by the RDKit	21831	9095	22408	20456	20521
conformers tethered by RDock	19861	5122	15255	10269	10209
poses obtained by docking	393620	102440	305100	205380	204180
poses minimized and scored after clustering (of X unique compounds)	202541 (2819)	85889 (636)	168680 (1997)	114293 (1290)	105264 (1254)

275 promiscuous fragments were discarded. This resulted in a
 276 number of fragment ranging from 137 (for BAZ2A) to 210 (for
 277 BRD4(1), Table 1). Interestingly, the numbers of fragments
 278 passing the filters reflect the druggability of the related
 279 bromodomains: BRD4(1) is considered the most promiscuous
 280 of the 61 human bromodomains, followed by CREBBP.³⁹
 281 BAZ2B is usually considered a difficult target,⁴⁰ but the fast
 282 growing number of binders^{7,41} would tend to rank it as a
 283 midrange druggability target. The bromodomains of BAZ2A
 284 and ATAD2 have been reported as very difficult targets.⁴² They
 285 were also the two bromodomains with the smallest number of
 286 fragments identified by ALTA-VS.

287 **Docking of Parent Compounds.** The number of parent
 288 compounds of the top ranking fragments ranged from 894 (for
 289 BAZ2A) to 2954 (for ATAD2) (Table 1). Docking was then
 290 carried out with RDock, a flexible docking software by tethering
 291 the fragment in the pose it had after SEED fragment docking.
 292 Diverse conformers of the parent compounds were generated
 293 with RDKit, using the ETKDG algorithm.⁴³ Fifty conformer
 294 generation runs were used per molecule and a threshold of
 295 diversity of 2 Å between conformers. Tethering was performed
 296 with the helper script of RDock, which relies partly on Open
 297 Babel, leading to some loss during the automatic detection of
 298 substructures in molecules. For flexible ligand docking, the
 299 binding site definition made use of a radius of 10 Å around each
 300 atom of the crystal ligand for all bromodomains except BAZ2A.
 301 Since BAZ2A had an acetylated peptide as ligand, we used the
 302 ligand of the closest analog, BAZ2B, after structural super-
 303 position. During the docking runs, the conserved water
 304 molecules were kept fixed and the compounds' head groups
 305 tethered as explained earlier. Other parameters were set as
 306 default. Twenty docking runs were carried out for each
 307 bromodomain/small molecule pair.

308 **Rescoring and Selection of Compounds.** Poses were
 309 clustered to avoid redundant binding modes with the RDKit
 310 (threshold of 1 Å) and converted to CHARMM file formats.
 311 Statistics on number of poses and compounds are in Table 1. A
 312 total of 676 667 poses were energy minimized by CHARMM
 313 which was used also to evaluate the electrostatic contribution to
 314 the binding free energy by finite-difference Poisson calculations.
 315 During minimization the bromodomain atoms and six
 316 conserved water molecules were kept rigid. The minimization
 317 protocol consisted of 500 steps of steepest descent followed by
 318 10 000 steps of conjugate gradient, with a tolerance of the
 319 energy gradient of 0.01 kcal/(mol Å). A distance-dependent
 320 dielectric constant of $4r$ (where r is the distance between
 321 atomic nuclei, i.e., positions of partial charges) was used during
 322 the minimization to avoid in vacuo minimization artifacts.^{44,45}
 323 The CHARMM pbeq module was used for the finite-difference
 324 Poisson calculations on the minimized structures.³³ The
 325 dielectric constant was set to 4.0 for the solute (bromodomain,
 326 six structural waters and ligand) and to 78.5 for the solvent.

The dielectric constant of 4.0 for the solute is a factor of 2.0
 larger than the one used for docking the fragments (in the
 generalized Born calculations in SEED). It was chosen to
 partially account for the flexibility of the ZA loop, which is
 more relevant for the docking of the parent compounds than
 the head-groups. The grid for the Poisson equation calculation
 was centered on the center of mass of the protein, with a
 nonfocused grid spacing of 1.0 Å and a focused grid spacing of
 0.3 Å. The number of grid points was automatically calculated
 in each dimension as $(40 + (X, Y, Z)_{\max} - (X, Y, Z)_{\min})/1.0$ for
 the nonfocused grid and $(10 + (X, Y, Z)_{\max} - (X, Y, Z)_{\min})/0.3$
 for the focused grid. The 40 and 33 (= 10/0.3) additional grid
 points in each dimension for the unfocused and focused grid,
 respectively, are required to extend the boundary by 20 and 5
 Å. The ionic strength was set to zero as it has little influence on
 the single point calculations of the binding free energy of
 protein–ligand complexes typical in pharmaceutical applica-
 tions.^{46–49} In the absence of an ionic atmosphere the Poisson–
 Boltzmann equation reduces to the Poisson equation. Similarly,
 no term was included for the nonpolar contribution to the free
 energy of solvation.^{50–54}

After energy minimization, some docked poses could move
 out of the asparagine subpocket because of unrealistically
 strained conformations or strongly unfavorable contacts. A filter
 was applied again to keep only compounds that interact with
 the conserved asparagine (distance <4.0 Å to the side chain
 nitrogen atom). Upon filtering, the top 100 compounds
 according to Delta electrostatics, and top 100 according to
 total energy efficiency were selected for each bromodomain.
 Some of these compounds were discarded as they contained
 chemotypes of known bromodomain inhibitors (e.g., dimethy-
 lisoxazole and acetylbenzene derivatives), or were commercially
 unavailable (in January 2016). Finally, 142 molecules (out of
 186) were selected for testing for ATAD2, 30 (of 65) for
 BAZ2A, 25 (of 67) for BAZ2B, 38 (of 152) for BRD4(1), and
 25 (of 163) for CREBBP (Table 2). Only a fraction of
 compounds were selected for the bromodomains of BRD4(1)
 and CREBBP as many of the top ranking compounds showed
 some similarity with known inhibitors of these two highly
 targeted bromodomains. Furthermore, for four of the five
 bromodomains several compounds were discarded because of
 close similarity among each other (e.g., pairs of molecules
 differing by a single halogen atom) while for ATAD2 almost all
 top ranking compounds were purchased because of the low
 druggability of this target and to generate some initial SAR. All
 the scoring and experimental data of the purchased compounds
 are available in the Supporting Information, section S5,
 including smiles chemical format depiction.

Validation Assays. Competition binding assays were
 performed to verify which compounds were true binders of
 their respective targets. Molecules were first tested in a single
 dose experiments at high concentration depending on the

Table 2. Summary of Experimental Results Per Target^a

	ATAD2	BAZ2A	BAZ2B	BRD4(1)	CREBBP	total
N tested	142	30	25	38	25	260
active in single dose	44	3	10	9	2	68
IC ₅₀ /K _D < 400 μM	19	0	2	3	2	26
IC ₅₀ /K _D < 100 μM	10	0	2	2	1	15
X-ray structures	N/A	1	2	N/A	N/A	3

^aActives in single dose were defined by using a threshold of less than 65% inhibition of the competitor ligand. Values of IC₅₀ were measured for ATAD2, BRD4(1), and CREBBP by AlphaScreen, while K_D values were measured for BAZ2A and BAZ2B by BROMOScan. X-ray crystallography was carried out only for the BAZ2A and BAZ2B bromodomains.

solubility (between 50 μM and 500 μM). In all cases, the DMSO concentration was 0.1%, except for ATAD2 for which it was 1%. ATAD2, BRD4(1), and CREBBP experiments were carried out by AlphaScreen assays⁵⁵ at Reaction Biology Corp. The AlphaScreen assay makes use of a donor bead (on the competitor molecule) that can transfer singlet oxygen to an acceptor bead (on the bromodomain target) when the two beads are in close proximity (<200 nm). The acceptor bead then emits a luminescent signal. When a compound binds the target, the donor/acceptor complex is disrupted, leading to a loss of singlet oxygen transfer and loss of the signal. The donor was histone H4 peptide (1–21) K5/8/12/16Ac-Biotin for ATAD2, CREBBP, and BRD4(1). The BAZ2A and BAZ2B assays were performed at DiscoverX with the BROMOScan profiling service.⁵⁶ The BROMOScan assay is a competition binding assay based on DNA-tagged bromodomain and quantitative PCR. The ligand used for the assay is proprietary and undisclosed.

The 68 compounds exhibiting a remnant binding of the competitor below 65% with respect to DMSO solution (Table 2) were considered for dose–response assays, i.e., determination of IC₅₀ (ATAD2, BRD4(1), and CREBBP at Reaction Biology Corp.) and K_D (BAZ2A and BAZ2B at DiscoverX) values. Out of these 68 molecules, the number was reduced to 39 mostly because of compound solubility, chemical novelty, and cost management. The binding affinity were investigated with the same assays as described before, with a curve fitting of 10-point dose responses for the AlphaScreen assay (ATAD2, BRD4(1), and CREBBP) and a curve fitting of 12-point dose responses in duplicates for the BROMOScan assay (BAZ2A, BAZ2B) (dose–response curves in the Supporting Information, section S3). Positives controls were as follows: JQ1⁵⁷ for ATAD2 (IC₅₀ = 64 μM) and BRD4(1) (IC₅₀ = 0.02 μM), SGC-CBP30⁵⁸ for CREBBP (IC₅₀ = 0.08 to 0.15 μM), and undisclosed for BAZ2A and BAZ2B.

It is important to provide evidence of specific binding for the active compounds. The 26 compounds that showed activity in dose–response assays were negative in tests for known pan-assay interference (PAINS) substructures at the FAF-Drugs4 Web server.⁵⁹ Furthermore, the 26 actives resulted negative in a test for known aggregation substructures or properties at the Aggregator Advisor Web server.⁶⁰

X-ray Crystallography. BAZ2A and BAZ2B bromodomains were produced and crystallized as described previously.⁶¹ Briefly, proteins were purified by IMAC, followed by buffer

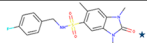
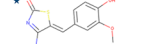
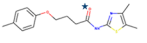
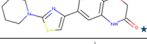

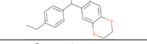
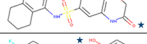
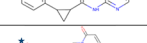

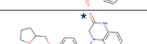
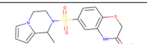
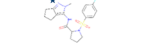
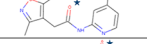
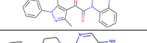
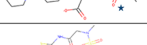

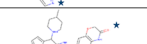
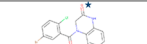
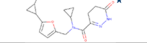

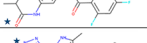


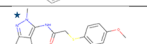
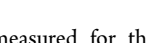
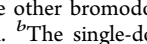
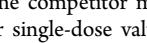
exchange, tag removal by TEV protease, a second IMAC and a size-exclusion chromatography. Complexes with the compounds of interest were obtained by cocrystallization for BAZ2A and by soaking for BAZ2B. Compounds were dissolved in the crystallization solution devoid of DMSO and MPD, which bind to the binding pocket of bromodomains.⁶² Diffraction data were collected at the Elettra Synchrotron Light Source (Trieste, Italy), XRD1 beamline (PDB codes 5OR8 and 5OR9) and at the Swiss Light Source, Paul Scherrer Institute (Villigen, Switzerland), beamline PXI (PDB code 5ORB). Data were processed with XDS⁶³ and Aimless;⁶⁴ high resolution cutoff was selected according to Karplus and Diederichs.⁶⁵ BAZ2B crystals soaked with compound 30 were strongly anisotropic: ellipsoidal diffraction data were treated making use of the STARANISO server (<http://staraniso.globalphasing.org/cgi-bin/staraniso.cgi>). Structures were solved by molecular replacement with Phaser⁶⁶ using PDB 4IRS as search model for BAZ2B and PDB 5MGJ for BAZ2A. Initial models were refined alternating cycles of automatic refinement with Phenix⁶⁷ and manual model building with COOT.⁶⁸

RESULTS AND DISCUSSION

ALTA-VS Identifies Binders for Four of the Five Bromodomains. The binding free energy of nearly 700 000 poses was evaluated upon minimization and finite-difference Poisson calculation of the electrostatic contribution to desolvation (see the Experimental Section). The top 25–38 compounds were selected for 4 of the 5 bromodomains, while 142 compounds were retained for ATAD2, which is a very difficult target.⁶⁹ Evaluation of the 260 compounds was performed by competition-binding assays (AlphaScreen at Reaction Biology Corp. and BROMOScan at DiscoverX). A total of 68 compounds (26%) showed less than 65% binding of the competitor molecule in single dose experiments at maximum dilution concentration (between 50 and 500 μM for most compounds). Thirty-nine of the 68 single-dose actives were evaluated in dose–response assays. The remaining 29 molecules were not considered further because of solubility and/or novelty considerations. Of the 39 single-dose actives that underwent dose–response measurements, 26 compounds showed an affinity below 400 μM, and 15 compounds below 100 μM (Table 2). Compound 30 showed significant inhibition of the BAZ2B bromodomain at a single dose of 50 μM but did not show activity in the dose–response assay. It is a competitive binder as its crystal structure in complex with BAZ2B confirmed that it binds in the pocket of the natural ligand (see below). The definition of an affinity threshold is not straightforward. It has been reported by several groups that the K_D values measured by the BROMOScan assay are up to an order of magnitude more favorable than the IC₅₀ values obtained by AlphaScreen.^{5,70–72} We decided to use the same threshold for both assays because most of the compounds (33 of 39) were evaluated by the AlphaScreen assay. If one excludes BAZ2A (see below), the success ratio (number of actives/number of tested molecules) ranged from 8% to 13% (19 binders of 142 compounds tested for ATAD2) with the 400-μM threshold and from 4% to 8% (2 binders of 25 compounds tested for BAZ2B) with the 100-μM threshold (Tables 2 and 3).

In addition to the 26 binders identified in dose–response measurements, we investigated the binding of compounds 1, 13, 30, 31, and 187 (Supporting Information section S4) by means of X-ray crystallography. These five compounds originate from the docking into BAZ2B and were tested by

Table 3. In Vitro Results for the 26 Compounds That Showed Activity in a Dose–Response Assay and Compound 30^b

Cpd	Target	Structure	% remnant inhibition of competitor at [μM]	IC ₅₀ μM	Calculated Delta electr. kcal/mol	Calculated total energy efficiency kcal/(mol HAC)	Calculated total energy kcal/mol
1	BAZ2B		1% 90 μM	6 ^a	2.7	-1.1	-27.5
2	BRD4(1)		38% 200 μM	22	0.9	-1.3	-21.4
3	ATAD2		10% 350 μM	23	-2.0	-0.9	-19.5
4	ATAD2		38% 50 μM	34	-1.6	-0.8	-17.8
5	ATAD2		40% 504 μM	34	-1.3	-0.9	-22.2
6	ATAD2		48% 504 μM	35	-1.4	-1.2	-28.6
7	BRD4(1)		23% 201 μM	37	0.4	-1.1	-27.8
8	ATAD2		4% 503 μM	44	-1.7	-1.3	-26.2
9	CREBBP		0% 503 μM	55	1.4	-1.1	-28.1
10	ATAD2		48% 318 μM	67	-0.9	-0.9	-22.0
11	ATAD2		48% 200 μM	70	-0.3	-1.0	-25.8
12	ATAD2		12% 479 μM	78	-2.4	-0.8	-19.5
13	BAZ2B		18% 160 μM	88 ^a	2.6	-1.2	-32.0
14	ATAD2		6% 503 μM	100	-0.3	-1.0	-17.2
15	ATAD2		29% 200 μM	100	0.4	-1.1	-31.6
16	ATAD2		37% 254 μM	151	0.9	-1.1	-28.3
17	ATAD2		42% 200 μM	151	0.4	-1.1	-22.0
18	BRD4(1)		40% 201 μM	167	-0.7	-1.6	-39.1
19	ATAD2		37% 399 μM	169	11.2	-1.2	-32.2
20	ATAD2		45% 504 μM	234	-1.1	-1.3	-26.3
21	ATAD2		47% 350 μM	248	-1.7	-0.8	-18.8
22	ATAD2		45% 350 μM	258	-0.3	-1.1	-27.7
23	ATAD2		43% 505 μM	288	0.0	-0.9	-20.1
24	CREBBP		31% 588 μM	336	-0.3	-0.9	-23.2
25	ATAD2		49% 504 μM	372	-0.5	-1.1	-27.0
26	ATAD2		49% 504 μM	396	2.3	-1.0	-20.2
30	BAZ2B		41% 50 μM	> 51	-0.3	-1.6	-35.7

^aAffinities measured for the BAZ2B bromodomain are K_D values, while for the other bromodomains, they are IC_{50} values measured by AlphaScreen. ^bThe single-dose value is the percentage of remaining binding of the competitor molecule with respect to DMSO solution; thus, smaller single-dose values reflect stronger binding of the tested molecule. The compounds are ordered according to the affinity. The star indicates the hydrogen bond acceptor that is predicted to be involved in the hydrogen bonds with the side chain of the conserved asparagine and the water molecule bridging to the conserved tyrosine. X-ray structures were solved for the complexes of compound 1 and

Table 3. continued

BAZ2A (PDB code 5OR8), compound 13 and BAZ2B (5OR9), and compound 30 and BAZB (5ORB).

crystallography in both BAZ2B and BAZ2A. These two 486
bromodomains share a very similar binding site, the only 487
difference being the gatekeeper residue (valine in BAZ2A, 488
isoleucine in BAZ2B).⁷³ Crystal structures of three of the five 489
molecules were determined: 1 in BAZ2A (2.4 Å resolution, 490
PDB code 5OR8), 13 and 30 in BAZ2B (2.0 Å resolution PDB 491
code 5OR9, and 2.1 Å resolution PDB code 5ORB, 492
respectively). The binding of 1 to BAZ2A is essentially 493
identical to the docking pose in BAZ2B (Figure 2, panel A). 494
The 1,3-dimethyl benzimidazolone headgroup is tilted as 495
compared to the docking pose, probably due to the difference 496
in the gatekeeper residue, as described in previous studies.^{61,74} 497
The crystal pose of the 1-methyl cyclopentapyrazole headgroup 498
of compound 13 displays similar contacts with the conserved 499
asparagine pocket as the docking pose but is less buried (Figure 500
2, panel B). The rest of the molecule is differently placed in the 501
crystal pose compared to the docking pose. This can be 502
ascribed to one or both of the following causes. First, the 503
electron density indicates that a single enantiomer is present, or 504
at least largely predominant, as already observed with other 505
compounds,^{7,41} while the other enantiomer was used for 506
docking. Second, crystal contacts may influence the binding 507
mode of the tail group. The fluorophenyl group of compound 508
13 is in van der Waals contact (3.5, 4.2, and 4.4 Å) with a 509
symmetric protein chain (Figure 2, panel C). Compound 30, 510
which contains the same 1-methyl cyclopentapyrazole head- 511
group as compound 13, has a binding mode essentially identical 512
in the crystal structure as in the docked pose. The main 513
difference between docking and crystal poses lays in the 514
position of the methoxybenzene tail, which is again in contact 515
with a symmetric unit in the crystal pose (4.4, 5.5, and 5.5 Å 516
contacts, Figure 2), at least in its most abundantly populated 517
orientation. Compounds 1 and 13 were confirmed binders in 518
dose–response measurements, unlike 30, which presented 519
interesting single-dose activity but was not confirmed in dose– 520
response measurement. The starting dilution for the dose– 521
response experiment of compound 30 was 50 μM, which is 522
much smaller than the millimolar concentration used for 523
soaking into BAZ2B. Furthermore, electron density is clearly 524
defined for compounds 1 and 13, while it strongly degrades in 525
the region of the methoxybenzene tail for compound 30, 526
indicating high mobility and/or multiple conformations for this 527
part of the molecule. Overall, the docking poses of the three 528
compounds are similar to the crystal poses: the headgroup is 529
correctly predicted and the main source of variability comes 530
from the tails which are partially solvent exposed and seem not 531
to interact specifically with the protein. 532

It is important to note that in vitro experiments were 533
performed on only 0.03% (for BAZ2B and CREBBP) to 0.2% 534
(for ATAD2) of the initial library (the nearly 77 000 535
compounds of the Lausanne Bioscreening Facility). In four 536
out of the five targets, micromolar binders were identified. For 537
the BAZ2A bromodomain, the three compounds that showed 538
activity in the single-dose measurement were not confirmed by 539
the dose–response assay. Out of any consideration of 540
druggability for this target, we discovered a posteriori a 541
nonoptimal preparation of the BAZ2A bromodomain structure. 542
The crucial water molecule that acts as hydrogen-bond bridge 543

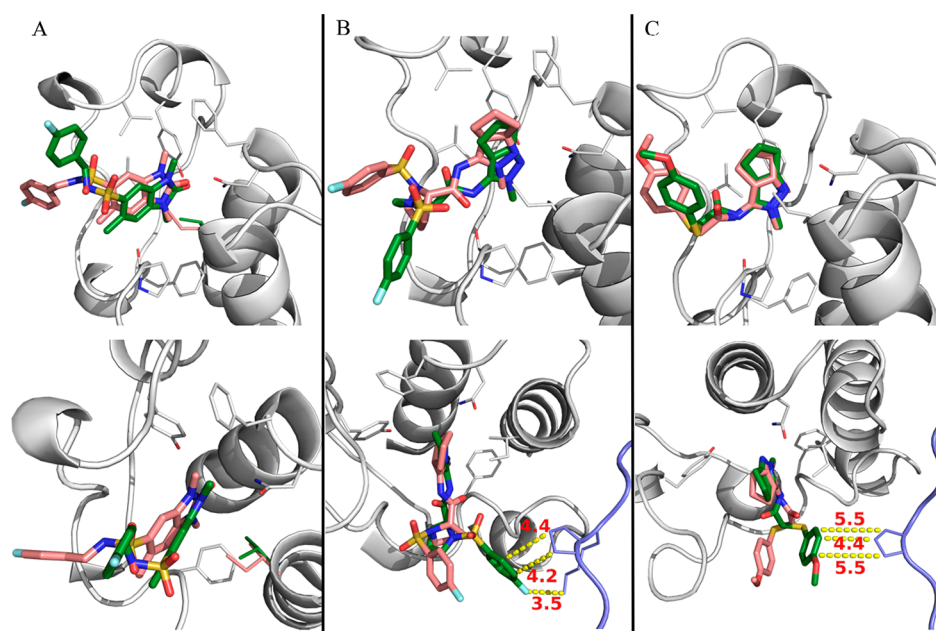


Figure 2. Comparison of binding modes from docking into BAZ2B (carbon atoms of ligands in salmon) and crystallography (carbon atoms of ligands in green). Two orientations are shown for each complex (top and bottom panels, respectively). van der Waals contacts (yellow dashed lines) with adjacent protein chains (blue) are labeled with the distance in angstroms (red). (A) Binding mode of compound **1**. The crystal pose has been solved in complex with BAZ2A (PDB code SOR8), while the docking pose originates from BAZ2B. The major difference in the binding pocket of BAZ2A versus BAZ2B is the gatekeeper residue: valine (green) in BAZ2A and isoleucine (salmon) in BAZ2B. The difference in bulkiness between these residues explains the tilt between head-groups observed in the bottom panel. (B) Binding mode of compound **13** in BAZ2B. A different stereoisomer has been docked than the one crystallized in BAZ2B (PDB code SOR9), which is also involved in crystal contacts (bottom part). The headgroup of the docking pose is slightly less buried than in the crystal structure. (C) Binding mode of compound **30** in BAZ2B. The crystal (PDB code SORB) and docking binding modes are essentially identical, with the main difference laying in the methoxybenzene tail, which contacts an adjacent protein chain of a crystal symmetric unit and is affected by a significant anisotropy (bottom part). All images were rendered using PyMOL, version 1.8.4, Schrödinger LLC.

544 to the side chain of the conserved tyrosine (Tyr1830) was
 545 protonated such that it could not allow for the water-mediated
 546 hydrogen bond (Figure 3). The failure on BAZ2A is due, at
 547 least in part, to the incorrect orientation of the structurally
 548 conserved water molecule as most crystal structures of
 549 complexes of bromodomain inhibitors provide evidence of its
 550 hydrogen-bond bridging role.⁷⁰ This interaction was unfortu-
 551 nately not possible in our structure. This points out again the

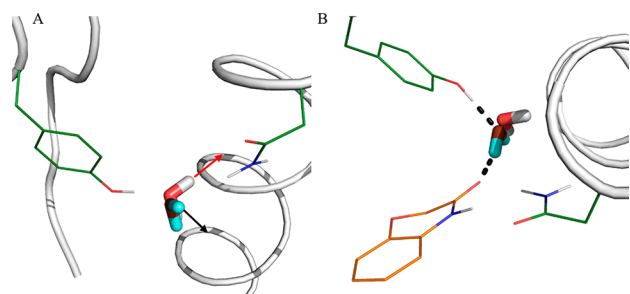


Figure 3. Orientation of the water molecule bridging to the conserved tyrosine in the structure prepared for BAZ2A (red and white sticks) vs the correct orientation as used for the other four bromodomains (purple and cyan sticks). (A) One of the two hydrogen atoms in the water of BAZ2A points toward the α -helix of the protein (red arrow) instead of pointing toward the solvent (black arrow). (B) The water molecule in the BAZ2A structure cannot act as hydrogen bond bridge with the side chain of the conserved tyrosine, a common feature found in most bromodomain inhibitors (one example is shown with carbon atoms in orange).

central importance of the preparation of the system for a virtual
 screening campaign, to the smallest details.⁷⁵

Two Energy Terms Used for Final Ranking Show Similar Predictive Ability. Consensus scoring has emerged as an interesting strategy to filter out false positive in virtual screening protocols.⁷⁶ Different scores are thought to compensate each other for their weaknesses. Here, we depart slightly from consensus scoring and make use of multiple ranking schemes according to individual energy contributions. Three different energy terms were used at the fragment selection stage and two of them are employed for the final ranking of the parent compounds. The three scores used, viz., Delta electrostatics, total energy efficiency, and electrostatic efficiency, favor different molecules. Delta electrostatics highlights the electrostatic complementarity between the receptor and the molecule and somewhat represents how better the molecule fits electrostatically in the protein environment rather than in water. Total energy efficiency favors molecules with a limited number of non-hydrogen atoms and is dominated by the steric complementarity between the ligand and the macromolecule (van der Waals interaction). Electrostatic efficiency emphasizes the direct electrostatic interaction between the ligand and the protein, in particular strong polar interactions such as charged contacts, weighted by the number of non-hydrogen atoms. Only Delta electrostatic and total energy efficiency were effectively used at the final compound selection step, electrostatic efficiency not selecting any unique molecule. In other words, all molecules selected because of electrostatic efficiency at the purchase stage were already, redundantly, chosen because of Delta electrostatics or total

energy efficiency. Of note, other combinations of scores and consensus scoring for fragments or compounds selection would also fit in the ALTA-VS strategy.

Inactive compounds (false positives in the ALTA-VS) were defined with a percentage of remnant binding between the competitor molecule and the protein of at least 65%. Binding molecules (true positives) were defined as those with an evaluated binding affinity (IC_{50} or K_D) and/or crystal structure, although not all molecules with a remnant substrate binding <65% were evaluated in dose–response assays. Of the 192 inactive compounds (i.e., false positives), 66 were chosen only because of Delta electrostatics, 60 because of total energy efficiency, and 66 were common to both energy terms used for ranking (Table 4 and Supporting Information, section S2).

Table 4. Analysis of Energy Terms Used for Ranking^a

	inactive in single-dose measurement (N = 192)	active in single-dose measurement (N = 68)	IC_{50} , K_D , or X_{tal} (N = 27)
chosen by Delta electrostatics	132	47	17
chosen by total energy efficiency	125	36	15
chosen <i>only</i> by Delta electrostatics	66	22	10
chosen <i>only</i> by total energy efficiency	60	15	10
chosen by both Delta electrostatics and total energy efficiency	66	31	7

^aA total of 260 molecules were tested in single-dose assays, which yielded 192 inactive compounds using a threshold of less than 65% remaining inhibition of the competitor ligand. Out of 68 molecules qualifying as active, 39 were chosen for dose–response assays, and 26 had a measurable IC_{50} (ATAD2, BRD4(1), or CREBBP) or K_D (BAZ2A or BAZ2B). In addition, compound 30 was not active in the dose–response assay (with a starting concentration of 50 μ M), but its structure in complex with its target bromodomain (BAZ2B) was solved.

Thus, the three possible combinations of the two energy terms tend to produce equally false positives. Interestingly, the same is observed for true positives. Of the 27 actives (26 dose–response actives and 1 dose–response inactive but with a crystal structure), 10 (37%) were selected only according to Delta electrostatics ranking, 10 (37%) only according to

energy efficiency, and 7 (26%) because of both terms (Table 4 and Supporting Information, section S2). Thus, the two energy terms used for the final selection of the compounds show similar sensitivity and specificity.

Advantages of Fragment-Tethered High-Throughput Docking.

The ALTA-VS protocol presented in this paper has several major advantages. The scoring of compounds includes solvation energies which is crucial to filter out false positives.¹³ The scoring function is based on a transferable force field and thus does not require a training set for fitting. Another pivotal asset is the placement of fragment head-groups in the binding pocket. Docking of rigid fragments decreases the complexity of the problem and allows for exhaustive sampling of the positions in the binding pocket. Placing fragments in binding pockets with SEED proved to have very good predictive power.^{5,7,9} Thanks to the correctly placed head-groups, the subsequent tethered docking also reduces the risks of failure by reducing the complexity of the sampling. Only conformations of the molecule around the tethered fragment need to be sampled and ranked. This step could be described as a fragment to hit expansion step. The goal is to grow from low affinity (i.e., high micromolar to millimolar) fragment binders to low micromolar hits whose potency can be interesting as starting points for further optimization in a medicinal chemistry pipeline.

Another big advantage of the ALTA-VS protocol is its cost and time efficiency. For each target, the small molecule library of nearly 77 000 compounds was investigated by docking only about 6000 fragments, followed by fragment-anchored docking of 1000 to 3000 parent molecules (more precisely 10 000 to 20 000 conformers), generating 100 000 to 200 000 poses for final minimization and finite-difference Poisson calculations (Table 1). If we consider a simple flexible docking protocol on the 77 000 molecules and extrapolate from our numbers, we would have ended up with roughly 10 million poses to be minimized per target, meaning an overall cost of ~50 million finite-difference Poisson single point calculations for this project. On a relatively small protein like a bromodomain, the ~50 million finite-difference Poisson calculations would have required ~1 to 2 million CPU h on a cluster with commodity processors (Xeon E3-1280 processors at 2.5 GHz in our study). Furthermore, it is important to note that the ALTA-VS relies solely on open-source/free for not-for-profit institutions software (Table 5), namely SEED (docking and scoring engine for fragments), RDock (flexible docking engine), CHARMM (scoring engine, in particular the version

Table 5. Software Used for the ALTA-VS^a

software	source type, licensing	ALTA-VS usage	link
RDKit	open source, Creative Commons Attribution–ShareAlike 4.0	small molecule calculations, data processing	http://www.rdkit.org/docs/Install.html
Open Babel	open source, GNU GPL	file handling	http://openbabel.org/wiki/Category:Installation
Marvin Suite (ChemAxon)	proprietary, free for noncommercial use	small molecule calculations	https://www.chemaxon.com/download/marvin-suite/
CGenFF	proprietary, permitted academic purpose	small molecule parametrization	https://www.paramchem.org/tech.php
SEED	binary executable free for all purpose	rigid docking, scoring	http://www.biochem-caflisch.uzh.ch/download/
RDock	open source, GNU LGPLv3	tethered flexible docking	http://rdock.sourceforge.net/download/
CHARMM	proprietary, free version without DOMDEC and GPU high performance modules for academic and nonprofit laboratories	minimization, scoring	http://charmm.chemistry.harvard.edu/charmm_lite.php

^aAll software are either free for academics and/or open source.

647 available at no cost for not-for-profit institutions), CGenFF
648 (small molecule parametrizer), RDKit (data processor), Open
649 Babel (data processor), and ChemAxon's Marvin Suite (small
650 molecule parameters calculator).

651 **Limitations.** There are limitations in the ALTA-VS
652 approach. Some are inherent to all virtual screening campaigns
653 and some are more specific (although not restricted) to our
654 (re)scoring scheme. First of all, as exemplified by the failed
655 BAZ2A campaign, the preparation of the input structures
656 (protein target, compound library) can strongly influence the
657 results. Furthermore, in most human bromodomains the
658 binding pocket for the natural ligand is rather small and rigid
659 and can be defined by one or two conserved residues, which is
660 not necessarily the case for other targets, e.g., proteases. For
661 those proteins with large and/or flexible binding site, the SEED
662 program could be used in a preprocessing step with a small
663 subset of fragments to target a broadly defined binding site
664 and/or multiple conformers originating from molecular
665 dynamics⁷⁷ or crystal structures.⁸ In this way, individual
666 subpockets with favorable binding energy for the probe
667 fragments could be identified from multiple structures. More
668 specifically to our protocol, the ALTA-VS is based on single-
669 point energy calculations; entropy and the contribution of
670 different metastable states (e.g., multiple orientations of the
671 nonanchor moiety) to the free energy of binding are neglected.
672 Additionally, the scoring relies on the continuum dielectric
673 approximation in both the fragment and full molecule stages.
674 Thus, it suffers from the theoretical limitations of such models,
675 like the depiction of the protein as a macroscopic dielectric
676 medium, the definition of the dielectric boundary, and the
677 disregard of nonpolar contributions to the hydration free
678 energy.⁷⁸ However, the assumptions made seem to be a good
679 compromise in terms of computational performance versus
680 quality of the scoring, when having to rescore hundreds of
681 thousands or even millions of poses.⁴⁴ Moreover, the quality of
682 the scoring calculations also depends on the quality of the force
683 field used. We used state of the art and fully consistent force
684 fields CHARMM36 for the protein¹⁵ and CHARMM
685 generalized force field (CGenFF)^{16,17} for all the fragments
686 and parent molecules of the library used for ALTA-VS.

687 ■ CONCLUSIONS

688 The number of commercially available small organic molecules
689 is growing steadily and is already close to one hundred
690 million.⁷⁹ Such continuous growth calls for efficient protocols
691 for in silico screening, particularly for protein structure-based
692 methods. The ALTA-VS protocol for fragment-anchored ligand
693 docking (Figure 1), introduced in 2005 and further improved
694 for the present application to bromodomains, combines the
695 advantages of docking with those of fragment-based ap-
696 proaches. Four main results emerge from the present study.
697 First, the updated ALTA-VS protocol is able to screen a library
698 of nearly 77 000 compounds (about 150 000 poses for energy
699 minimization, Table 1) within 2 days of computational time on
700 a 96-core compute cluster (equipped with Xeon E3-1280 quad
701 core processors at 2.5 GHz). Most of the computational time is
702 required for energy minimization of the docked poses and
703 evaluation of electrostatic solvation by the finite-difference
704 Poisson equation which require around 1.5 min per pose.
705 Overall, the ALTA-VS has identified ligands for four
706 bromodomains (Table 2). More precisely, 15 of the 39
707 compounds for which dose–response measurements were
708 performed have an affinity of 100 μM or better (Table 3).

Second, the application of the updated ALTA-VS protocol 709
provides evidence of the usefulness of the novel aspects. 710
Retrospectively, the use of a single anchor fragment in the 711
updated ALTA-VS protocol has resulted in 15 active molecules 712
(out of 27) consisting of only two ring systems. These ligands 713
would not have been identified by the original version of 714
ALTA-VS, which required three anchor fragments. Further- 715
more, most of these ligands have only one ring system (the 716
headgroup) fully buried in the bromodomain binding site while 717
the tail groups are rather flexible and can assume multiple 718
orientations which is not congruent with the role of anchor 719
fragment. Another new aspect of the updated ALTA-VS 720
protocol is the use of a transferable force field without any 721
fitting parameter. The paucity of known inhibitors of the 722
ATAD2 bromodomain would have hindered the derivation of 723
the fitting parameters which was necessary in the original 724
ALTA-VS protocol. 725

Third, the preparation of the protein structure used for 726
docking is a crucial step. In the ALTA-VS campaign for BAZ2A, 727
the incorrect orientation of a structurally conserved water 728
molecule (Figure 3) resulted in a more poor outcome than for 729
the other four bromodomains for which the orientation of the 730
conserved water was correct. This water molecule acts as 731
hydrogen bond-bridge between a conserved tyrosine side chain 732
and the natural ligand (acetylated lysine) or the large majority 733
of known inhibitors. The correct orientation of the water 734
hydrogens plays a critical role because the electrostatic energy, 735
which is based on partial charges, is very sensitive on the 736
position and orientations of dipoles, and the water molecule has 737
a strong dipole moment of 2.35 D in the force field used in this 738
work. 739

Fourth, two different energy terms were used for the final 740
selection of compounds: Delta electrostatics (i.e., the protein/ 741
ligand electrostatic interaction minus the free energy of 742
hydration) and total binding energy divided by the number 743
of non-hydrogen atoms. These terms showed similar predictive 744
ability (Table 4). More precisely, selection of compounds for in 745
vitro testing by either of the two terms (or both) resulted in a 746
similar amount of true positives (sensitivity) and similar 747
numbers of false positives (specificity). 748

In conclusion, the present study and our previous 749
applications of the ALTA-VS protocol^{10–14} provide strong 750
evidence of the usefulness and efficiency of fragment-anchored 751
docking of flexible molecules for in silico screening. The ALTA- 752
VS protocol can be employed also for screening for covalent 753
binders by replacing tethered docking with covalent docking. If 754
experimental binding modes of fragment hits are available, they 755
can be integrated in the protocol and replace docked pose for 756
tethered docking. Since the updated version of the ALTA-VS 757
makes use of a transferable force field and does not require any 758
training set for fitting parameters, it should be applicable to 759
most target proteins of known three-dimensional structure. It 760
also has the notable advantage to be based solely on open 761
source and/or free for academics software. 762

■ ASSOCIATED CONTENT

Supporting Information

The Supporting Information is available free of charge on the 765
ACS Publications website at DOI: 10.1021/acs.jcim.7b00336. 766

Detailed description of the screening library, details of 767
docking scores with respect to experimental data, 768
Alphascreen/BROMOScan dose–response curves, X-ray 769

770 crystallization data, docking and experimental data for all
771 tested molecules (PDF)

772 ■ AUTHOR INFORMATION

773 Corresponding Author

774 *Phone: (+41 44) 635 55 21. Fax: (+41 44) 635 68 62. E-mail:
775 caflisch@bioc.uzh.ch.

776 ORCID

777 Jean-Rémy Marchand: [0000-0002-8002-9457](https://orcid.org/0000-0002-8002-9457)

778 Amedeo Caflisch: [0000-0002-2317-6792](https://orcid.org/0000-0002-2317-6792)

779 Author Contributions

780 The study was designed by J.R.M. and A.C. J.R.M. performed
781 the docking. J.R.M. and A.C. analyzed the docking results.
782 A.D.V. and G.L. carried out the crystallography. The manu-
783 script was written by J.R.M. and A.C. All authors have given
784 approval to the final version of the manuscript.

785 Funding

786 Swiss Cancer Society (Krebsliga Schweiz, grant Nr. KLS-3098-
787 02-2013).

788 Notes

789 The authors declare no competing financial interest.

790 ■ ACKNOWLEDGMENTS

791 The authors thank Carmen Esposito, Nicholas Deerain, and Dr.
792 Dimitrios Spiliotopoulos for compound ordering and handling.
793 The authors also thank the anonymous reviewers for their
794 valuable comments that helped improve the clarity and scope of
795 the manuscript.

796 ■ ABBREVIATIONS

797 ALTA-VS, anchor-based library tailoring approach for virtual
798 screening; ATAD2, ATPase family AAA domain containing 2;
799 BAZ2A, bromodomain adjacent to zinc finger domain 2A;
800 BAZ2B, bromodomain adjacent to zinc finger domain 2B;
801 BRD4(1), bromodomain-containing protein 4, bromodomain
802 1; CREBBP, cAMP response element binding protein binding
803 protein; DMSO, dimethyl sulfoxide; IMAC, immobilized metal
804 ion affinity chromatography; MPD, 2-methyl-2,4-pentandiol;
805 TEV protease, tobacco etch virus nuclear-inclusion-a endopep-
806 tidase

807 ■ REFERENCES

808 (1) Erlanson, D. A.; Fesik, S. W.; Hubbard, R. E.; Jahnke, W.; Jhoti,
809 H. Twenty Years on: The Impact of Fragments on Drug Discovery.
810 *Nat. Rev. Drug Discovery* **2016**, *15*, 605–619.
811 (2) Irwin, J. J.; Shoichet, B. K. Docking Screens for Novel Ligands
812 Conferring New Biology. *J. Med. Chem.* **2016**, *59*, 4103–4120.
813 (3) Seifert, M. H. J.; Wolf, K.; Vitt, D. Virtual High-Throughput In
814 Silico Screening. *BIO SILICO* **2003**, *1*, 143–149.
815 (4) Doman, T. N.; McGovern, S. L.; Witherbee, B. J.; Kasten, T. P.;
816 Kurumbail, R.; Stallings, W. C.; Connolly, D. T.; Shoichet, B. K.
817 Molecular Docking and High-Throughput Screening for Novel
818 Inhibitors of Protein Tyrosine Phosphatase-1B. *J. Med. Chem.* **2002**,
819 *45*, 2213–2221.
820 (5) Spiliotopoulos, D.; Zhu, J.; Wamhoff, E. C.; Deerain, N.;
821 Marchand, J. R.; Aretz, J.; Rademacher, C.; Caflisch, A. Virtual Screen
822 to NMR (VS2NMR): Discovery of Fragment Hits for the CBP
823 Bromodomain. *Bioorg. Med. Chem. Lett.* **2017**, *27*, 2472–2478.
824 (6) Steinbrecher, T. B.; Dahlgren, M.; Cappel, D.; Lin, T.; Wang, L.;
825 Krilov, G.; Abel, R.; Friesner, R.; Sherman, W. Accurate Binding Free
826 Energy Predictions in Fragment Optimization. *J. Chem. Inf. Model.*
827 **2015**, *55*, 2411–2420.

(7) Lolli, G.; Caflisch, A. High-Throughput Fragment Docking into 828
the BAZ2B Bromodomain: Efficient in Silico Screening for X-Ray 829
Crystallography. *ACS Chem. Biol.* **2016**, *11*, 800–807. 830
(8) Xu, M.; Unzue, A.; Dong, J.; Spiliotopoulos, D.; Nevado, C.; 831
Caflisch, A. Discovery of CREBBP Bromodomain Inhibitors by High- 832
Throughput Docking and Hit Optimization Guided by Molecular 833
Dynamics. *J. Med. Chem.* **2016**, *59*, 1340–1349. 834
(9) Zhu, J.; Caflisch, A. Twenty Crystal Structures of Bromodomain 835
and PHD Finger Containing Protein 1 (BRPF1)/Ligand Complexes 836
Reveal Conserved Binding Motifs and Rare Interactions. *J. Med. Chem.* 837
2016, *59*, 5555–5561. 838
(10) Huang, D.; Luthi, U.; Kolb, P.; Cecchini, M.; Barberis, A.; 839
Caflisch, A. In Silico Discovery of Beta-Secretase Inhibitors. *J. Am.* 840
Chem. Soc. **2006**, *128*, 5436–5443. 841
(11) Huang, D.; Luthi, U.; Kolb, P.; Edler, K.; Cecchini, M.; Audetat, 842
S.; Barberis, A.; Caflisch, A. Discovery of Cell-Permeable non-Peptide 843
Inhibitors of Beta-Secretase by High-Throughput Docking and 844
Continuum Electrostatics Calculations. *J. Med. Chem.* **2005**, *48*, 845
5108–5111. 846
(12) Kolb, P.; Kipouros, C. B.; Huang, D.; Caflisch, A. Structure- 847
Based Tailoring of Compound Libraries for High-Throughput 848
Screening: Discovery of Novel EphB4 Kinase Inhibitors. *Proteins: 849*
Struct., Funct., Genet. **2008**, *73*, 11–18. 850
(13) Kolb, P.; Huang, D.; Dey, F.; Caflisch, A. Discovery of Kinase 851
Inhibitors by High-Throughput Docking and Scoring Based on a 852
Transferable Linear Interaction Energy Model. *J. Med. Chem.* **2008**, *51*, 853
1179–1188. 854
(14) Schenker, P.; Alfarano, P.; Kolb, P.; Caflisch, A.; Baici, A. A 855
Double-Headed Cathepsin B Inhibitor Devoid of Warhead. *Protein Sci.* 856
2008, *17*, 2145–2155. 857
(15) Best, R. B.; Zhu, X.; Shim, J.; Lopes, P. E.; Mittal, J.; Feig, M.; 858
Mackerell, A. D., Jr. Optimization of the Additive CHARMM All-Atom 859
Protein Force Field Targeting Improved Sampling of the Backbone 860
Phi, Psi and Side-Chain Chi(1) and Chi(2) Dihedral Angles. *J. Chem.* 861
Theory Comput. **2012**, *8*, 3257–3273. 862
(16) Vanommeslaeghe, K.; MacKerell, A. D., Jr. Automation of the 863
CHARMM General Force Field (CGenFF) I: Bond Perception and 864
Atom Typing. *J. Chem. Inf. Model.* **2012**, *52*, 3144–3154. 865
(17) Vanommeslaeghe, K.; Raman, E. P.; MacKerell, A. D., Jr. 866
Automation of the CHARMM General Force Field (CGenFF) II: 867
Assignment of Bonded Parameters and Partial Atomic Charges. *J.* 868
Chem. Inf. Model. **2012**, *52*, 3155–3168. 869
(18) Filippakopoulos, P.; Picaud, S.; Mangos, M.; Keates, T.; 870
Lambert, J. P.; Barsyte-Lovejoy, D.; Felletar, I.; Volkmer, R.; Muller, S.; 871
Pawson, T.; Gingras, A. C.; Arrowsmith, C. H.; Knapp, S. Histone 872
Recognition and Large-Scale Structural Analysis of the Human 873
Bromodomain Family. *Cell* **2012**, *149*, 214–231. 874
(19) Marchand, J. R.; Caflisch, A. Binding Mode of Acetylated 875
Histones to Bromodomains: Variations on a Common Motif. 876
ChemMedChem **2015**, *10*, 1327–1333. 877
(20) Fujisawa, T.; Filippakopoulos, P. Functions of Bromodomain- 878
Containing Proteins and their Roles in Homeostasis and Cancer. *Nat.* 879
Rev. Mol. Cell Biol. **2017**, *18*, 246–262. 880
(21) United States National Library of Medicine. www.clinicaltrials.gov. 881
882
(22) Theodoulou, N. H.; Tomkinson, N. C. O.; Prinjha, R. K.; 883
Humphreys, P. G. Clinical Progress and Pharmacology of Small 884
Molecule Bromodomain Inhibitors. *Curr. Opin. Chem. Biol.* **2016**, *33*, 885
58–66. 886
(23) Muller, S.; Filippakopoulos, P.; Knapp, S. Bromodomains as 887
Therapeutic Targets. *Expert Rev. Mol. Med.* **2011**, *13*, e29. 888
(24) Unzue, A.; Lafleur, K.; Zhao, H.; Zhou, T.; Dong, J.; Kolb, P.; 889
Liebl, J.; Zahler, S.; Caflisch, A.; Nevado, C. Three Stories on Eph 890
Kinase Inhibitors: From In Silico Discovery to In Vivo Validation. 891
J. Med. Chem. **2016**, *112*, 347–366. 892
(25) Zhao, H.; Caflisch, A. Molecular Dynamics in Drug Design. *Eur.* 893
J. Med. Chem. **2015**, *91*, 4–14. 894

- 895 (26) Majeux, N.; Scarsi, M.; Apostolakis, J.; Ehrhardt, C.; Cafilisch, A.
896 Exhaustive Docking of Molecular Fragments with Electrostatic
897 Solvation. *Proteins: Struct., Funct., Genet.* **1999**, *37*, 88–105.
- 898 (27) Majeux, N.; Scarsi, M.; Cafilisch, A. Efficient Electrostatic
899 Solvation Model for Protein-Fragment Docking. *Proteins: Struct.,
900 Funct., Genet.* **2001**, *42*, 256–268.
- 901 (28) Scarsi, M.; Apostolakis, J.; Cafilisch, A. Continuum Electrostatic
902 Energies of Macromolecules in Aqueous Solutions. *J. Phys. Chem. A*
903 **1997**, *101*, 8098–8106.
- 904 (29) Ruiz-Carmona, S.; Alvarez-Garcia, D.; Foloppe, N.; Garmendia-
905 Doval, A. B.; Juhos, S.; Schmidtke, P.; Barril, X.; Hubbard, R. E.;
906 Morley, S. D. rDock: A Fast, Versatile and Open Source Program for
907 Docking Ligands to Proteins and Nucleic Acids. *PLoS Comput. Biol.*
908 **2014**, *10*, 10.
- 909 (30) Cecchini, M.; Kolb, P.; Majeux, N.; Cafilisch, A. Automated
910 Docking of Highly Flexible Ligands by Genetic Algorithms: A Critical
911 Assessment. *J. Comput. Chem.* **2004**, *25*, 412–422.
- 912 (31) Budin, N.; Majeux, N.; Cafilisch, A. Fragment-Based Flexible
913 Ligand Docking by Evolutionary Optimization. *Biol. Chem.* **2001**, *382*,
914 1365–1372.
- 915 (32) Vidler, L. R.; Brown, N.; Knapp, S.; Hoelder, S. Druggability
916 Analysis and Structural Classification of Bromodomain Acetyl-lysine
917 Binding Sites. *J. Med. Chem.* **2012**, *55*, 7346–7359.
- 918 (33) Im, W.; Beglov, D.; Roux, B. Continuum Solvation Model:
919 Computation of Electrostatic Forces from Numerical Solutions to the
920 Poisson-Boltzmann Equation. *Comput. Phys. Commun.* **1998**, *111*, 59–
921 75.
- 922 (34) Brooks, B. R.; Brooks, C. L.; Mackerell, A. D.; Nilsson, L.;
923 Petrella, R. J.; Roux, B.; Won, Y.; Archontis, G.; Bartels, C.; Boresch,
924 S.; Cafilisch, A.; Caves, L.; Cui, Q.; Dinner, A. R.; Feig, M.; Fischer, S.;
925 Gao, J.; Hodoseck, M.; Im, W.; Kuczera, K.; Lazaridis, T.; Ma, J.;
926 Ovchinnikov, V.; Paci, E.; Pastor, R. W.; Post, C. B.; Pu, J. Z.; Schaefer,
927 M.; Tidor, B.; Venable, R. M.; Woodcock, H. L.; Wu, X.; Yang, W.;
928 York, D. M.; Karplus, M. CHARMM: The Biomolecular Simulation
929 Program. *J. Comput. Chem.* **2009**, *30*, 1545–1614.
- 930 (35) EPFL Biomolecular Screening Facility, BSF-ACCESS Chemicals
931 Collections. <http://bsf.epfl.ch/collections#faq-568582>.
- 932 (36) ChemAxon Prediction of dissociation constant using micro-
933 constants. [https://docs.chemaxon.com/download/attachments/
934 41128347/Prediction_of_dissociation_constant_using_
935 microconstants.pdf](https://docs.chemaxon.com/download/attachments/41128347/Prediction_of_dissociation_constant_using_microconstants.pdf).
- 936 (37) Landrum, G. RDKit: Open-source cheminformatics. rdkit.org.
- 937 (38) O'Boyle, N. M.; Banck, M.; James, C. A.; Morley, C.;
938 Vandermeersch, T.; Hutchison, G. R. Open Babel: An Open Chemical
939 Toolbox. *J. Cheminf.* **2011**, *3*, 33.
- 940 (39) Filippakopoulos, P.; Knapp, S. Targeting Bromodomains:
941 Epigenetic Readers of Lysine Acetylation. *Nat. Rev. Drug Discovery*
942 **2014**, *13*, 337–356.
- 943 (40) Ferguson, F. M.; Fedorov, O.; Chaikuad, A.; Philpott, M.;
944 Muniz, J. R.; Felletar, I.; von Delft, F.; Heightman, T.; Knapp, S.; Abell,
945 C.; Ciulli, A. Targeting Low-Druggability Bromodomains: Fragment
946 Based Screening and Inhibitor Design against the BAZ2B
947 Bromodomain. *J. Med. Chem.* **2013**, *56*, 10183–10187.
- 948 (41) Marchand, J. R.; Lolli, G.; Cafilisch, A. Derivatives of 3-Amino-2-
949 Methylpyridine as BAZ2B Bromodomain Ligands: In Silico Discovery
950 and in Crystallo Validation. *J. Med. Chem.* **2016**, *59*, 9919–9927.
- 951 (42) Chaikuad, A.; Petros, A. M.; Fedorov, O.; Xu, J.; Knapp, S.
952 Structure-Based Approaches towards Identification of Fragments for
953 the Low-Druggability ATAD2 Bromodomain. *MedChemComm* **2014**,
954 *5*, 1843–1848.
- 955 (43) Riniker, S.; Landrum, G. A. Better Informed Distance
956 Geometry: Using what we Know to Improve Conformation
957 Generation. *J. Chem. Inf. Model.* **2015**, *55*, 2562–2574.
- 958 (44) Foloppe, N.; Hubbard, R. Towards Predictive Ligand Design
959 with Free-Energy Based Computational Methods? *Curr. Med. Chem.*
960 **2006**, *13*, 3583–3608.
- 961 (45) Hunenberger, P. H.; Helms, V.; Narayana, N.; Taylor, S. S.;
962 McCammon, J. A. Determinants of Ligand Binding to cAMP-
963 Dependent Protein Kinase. *Biochemistry* **1999**, *38*, 2358–2366.
- (46) Froloff, N.; Windemuth, A.; Honig, B. On the Calculation of 964
Binding Free Energies Using Continuum Methods: Application to 965
MHC Class I Protein-Peptide Interactions. *Protein Sci.* **1997**, *6*, 1293–
966 1301.
- (47) Huo, S.; Wang, J.; Cieplak, P.; Kollman, P. A.; Kuntz, I. D. 967
Molecular dynamics and Free Energy Analyses of Cathepsin D- 968
Inhibitor Interactions: Insight into Structure-Based Ligand Design. *J.* 969
Med. Chem. **2002**, *45*, 1412–1419. 970
- (48) Schwarzl, S. M.; Tschopp, T. B.; Smith, J. C.; Fischer, S. Can the 971
Calculation of Ligand Binding Free Energies be Improved with 972
Continuum Solvent Electrostatics and an Ideal-Gas Entropy 973
Correction? *J. Comput. Chem.* **2002**, *23*, 1143–1149. 974
- (49) Shen, J.; Wendoloski, J. Electrostatic Binding Energy 975
Calculation Using the Finite Difference Solution to the Linearized 976
Poisson-Boltzmann Equation: Assessment of its Accuracy. *J. Comput.* 977
Chem. **1996**, *17*, 350–357. 978
- (50) Czaplewski, C.; Ripoll, D. R.; Liwo, A.; Rodziewicz-Motowidlo, 979
S.; Wawak, R. J.; Scheraga, H. A. Can Cooperativity in Hydrophobic 980
Association Be Reproduced Correctly by Implicit Solvation Models? 981
Int. J. Quantum Chem. **2002**, *88*, 41–55. 982
- (51) Feig, M.; Brooks, C. L. Recent Advances in the Development 983
and Application of Implicit Solvent Models in Biomolecule 984
Simulations. *Curr. Opin. Struct. Biol.* **2004**, *14*, 217–224. 985
- (52) Levy, R. M.; Zhang, L. Y.; Gallicchio, E.; Felts, A. K. On the 986
Nonpolar Hydration Free Energy of Proteins: Surface Area and 987
Continuum Solvent Models for the Solute-Solvent Interaction Energy. 988
J. Am. Chem. Soc. **2003**, *125*, 9523–9530. 989
- (53) Pitera, J. W.; van Gunsteren, W. F. The Importance of Solute- 990
Solvent Van Der Waals Interactions with Interior Atoms of 991
Biopolymers. *J. Am. Chem. Soc.* **2001**, *123*, 3163–3164. 992
- (54) Shimizu, S.; Chan, H. S. Anti-Cooperativity and Cooperativity 993
in Hydrophobic Interactions: Three-Body Free Energy Landscapes 994
and Comparison with Implicit-Solvent Potential Functions for 995
Proteins. *Proteins: Struct., Funct., Genet.* **2002**, *48*, 15–30. 996
- (55) Philpott, M.; Yang, J.; Tumber, T.; Fedorov, O.; Uttarkar, S.; 997
Filippakopoulos, P.; Picaud, S.; Keates, T.; Felletar, I.; Ciulli, A.; 998
Knapp, S.; Heightman, T. D. Bromodomain-Peptide Displacement 999
Assays for Interactome Mapping and Inhibitor Discovery. *Mol. BioSyst.* 1000
2011, *7*, 2899–2908. 1001
- (56) Quinn, E.; Wodicka, L.; Ciceri, P.; Pallares, G.; Pickle, E.; 1002
Torrey, A.; Floyd, M.; Hunt, J.; Treiber, D. Abstract 4238: 1003
BROMOScan - a High Throughput, Quantitative Ligand Binding 1004
Platform Identifies Best-in-Class Bromodomain Inhibitors from a 1005
Screen of Mature Compounds Targeting other Protein Classes. *Cancer* 1006
Res. **2013**, *73*, 4238. 1007
- (57) Filippakopoulos, P.; Qi, J.; Picaud, S.; Shen, Y.; Smith, W. B.; 1008
Fedorov, O.; Morse, E. M.; Keates, T.; Hickman, T. T.; Felletar, I.; 1009
Philpott, M.; Munro, S.; McKeown, M. R.; Wang, Y.; Christie, A. L.; 1010
West, N.; Cameron, M. J.; Schwartz, B.; Heightman, T. D.; La 1011
Thangue, N.; French, C. A.; Wiest, O.; Kung, A. L.; Knapp, S.; 1012
Bradner, J. E. Selective Inhibition of BET Bromodomains. *Nature* 1013
2010, *468*, 1067–1073. 1014
- (58) Hammitzsch, A.; Tallant, C.; Fedorov, O.; O'Mahony, A.; 1015
Brennan, P. E.; Hay, D. A.; Martinez, F. O.; Al-Mossawi, M. H.; de 1016
Wit, J.; Vecellio, M.; Wells, C.; Wordsworth, P.; Muller, S.; Knapp, S.; 1017
Bowness, P. CBP30, a Selective CBP/p300 Bromodomain Inhibitor, 1018
Suppresses Human Th17 Responses. *Proc. Natl. Acad. Sci. U. S. A.* 1019
2015, *112*, 10768–10773. 1020
- (59) Lagorce, D.; Sperandio, O.; Baell, J. B.; Miteva, M. A.; 1021
Villoutreix, B. O. FAF-Drugs3: A Web Server for Compound Property 1022
Calculation and Chemical Library Design. *Nucleic Acids Res.* **2015**, *43*,
1023 W200–W207. 1024
- (60) Irwin, J. J.; Duan, D.; Torosyan, H.; Doak, A. K.; Ziebart, K. T.; 1025
Sterling, T.; Tumanian, G.; Shoichet, B. K. An Aggregation Advisor for 1026
Ligand Discovery. *J. Med. Chem.* **2015**, *58*, 7076–7087. 1027
- (61) Spiliotopoulos, D.; Wamhoff, E.-C.; Lolli, G.; Rademacher, C.; 1028
Cafilisch, A. Discovery of BAZ2A Bromodomain Ligands. *Eur. J. Med.* 1029
Chem. **2017**, DOI: 10.1016/j.ejmech.2017.08.028. 1030

- 1032 (62) Lolli, G.; Battistutta, R. Different Orientations of Low-
1033 Molecular-Weight Fragments in the Binding Pocket of a BRD4
1034 Bromodomain. *Acta Crystallogr., Sect. D: Biol. Crystallogr.* **2013**, *69*,
1035 2161–2164.
- 1036 (63) Kabsch, W. Xds. *Acta Crystallogr., Sect. D: Biol. Crystallogr.* **2010**,
1037 *66*, 125–132.
- 1038 (64) Evans, P. R.; Murshudov, G. N. How Good Are my Data and
1039 What Is the Resolution? *Acta Crystallogr., Sect. D: Biol. Crystallogr.*
1040 **2013**, *69*, 1204–1214.
- 1041 (65) Karplus, P. A.; Diederichs, K. Assessing and Maximizing Data
1042 Quality in Macromolecular Crystallography. *Curr. Opin. Struct. Biol.*
1043 **2015**, *34*, 60–68.
- 1044 (66) McCoy, A. J.; Grosse-Kunstleve, R. W.; Adams, P. D.; Winn, M.
1045 D.; Storoni, L. C.; Read, R. J. Phaser Crystallographic Software. *J. Appl.*
1046 *Crystallogr.* **2007**, *40*, 658–674.
- 1047 (67) Adams, P. D.; Afonine, P. V.; Bunkoczi, G.; Chen, V. B.; Davis,
1048 I. W.; Echols, N.; Headd, J. J.; Hung, L. W.; Kapral, G. J.; Grosse-
1049 Kunstleve, R. W.; McCoy, A. J.; Moriarty, N. W.; Oeffner, R.; Read, R.
1050 J.; Richardson, D. C.; Richardson, J. S.; Terwilliger, T. C.; Zwart, P. H.
1051 PHENIX: a Comprehensive Python-Based System for Macro-
1052 molecular Structure Solution. *Acta Crystallogr., Sect. D: Biol. Crystallogr.*
1053 **2010**, *66*, 213–221.
- 1054 (68) Emsley, P.; Lohkamp, B.; Scott, W. G.; Cowtan, K. Features and
1055 Development of Coot. *Acta Crystallogr., Sect. D: Biol. Crystallogr.* **2010**,
1056 *66*, 486–501.
- 1057 (69) Bamborough, P.; Chung, C. W.; Demont, E. H.; Furze, R. C.;
1058 Bannister, A. J.; Che, K. H.; Diallo, H.; Douault, C.; Grandi, P.;
1059 Kouzarides, T.; Michon, A. M.; Mitchell, D. J.; Prinjha, R. K.; Rau, C.;
1060 Robson, S.; Sheppard, R. J.; Upton, R.; Watson, R. J. A Chemical
1061 Probe for the ATAD2 Bromodomain. *Angew. Chem., Int. Ed.* **2016**, *55*,
1062 11382–11386.
- 1063 (70) Crawford, T. D.; Tsui, V.; Flynn, E. M.; Wang, S.; Taylor, A. M.;
1064 Cote, A.; Audia, J. E.; Beresini, M. H.; Burdick, D. J.; Cummings, R.;
1065 Dakin, L. A.; Duplessis, M.; Good, A. C.; Hewitt, M. C.; Huang, H. R.;
1066 Jayaram, H.; Kiefer, J. R.; Jiang, Y.; Murray, J.; Nasveschuk, C. G.;
1067 Pardo, E.; Poy, F.; Romero, F. A.; Tang, Y.; Wang, J.; Xu, Z.;
1068 Zawadzke, L. E.; Zhu, X.; Albrecht, B. K.; Magnuson, S. R.; Bellon, S.;
1069 Cochran, A. G. Diving into the Water: Inducible Binding
1070 Conformations for BRD4, TAF1(2), BRD9, and CECR2 Bromodo-
1071 mains. *J. Med. Chem.* **2016**, *59*, 5391–5402.
- 1072 (71) Tanaka, M.; Roberts, J. M.; Seo, H. S.; Souza, A.; Paulk, J.; Scott,
1073 T. G.; DeAngelo, S. L.; Dhe-Paganon, S.; Bradner, J. E. Design and
1074 Characterization of Bivalent BET Inhibitors. *Nat. Chem. Biol.* **2016**, *12*,
1075 1089–1096.
- 1076 (72) Theodoulou, N. H.; Bamborough, P.; Bannister, A. J.; Becher, L.;
1077 Bit, R. A.; Che, K. H.; Chung, C. W.; Dittmann, A.; Drewes, G.;
1078 Drewry, D. H.; Gordon, L.; Grandi, P.; Leveridge, M.; Lindon, M.;
1079 Michon, A. M.; Molnar, J.; Robson, S. C.; Tomkinson, N. C. O.;
1080 Kouzarides, T.; Prinjha, R. K.; Humphreys, P. G. Discovery of I-BRD9,
1081 a Selective Cell Active Chemical Probe for Bromodomain Containing
1082 Protein 9 Inhibition. *J. Med. Chem.* **2016**, *59*, 1425–1439.
- 1083 (73) Flynn, E. M.; Huang, O. W.; Poy, F.; Oppikofer, M.; Bellon, S.
1084 F.; Tang, Y.; Cochran, A. G. A Subset of Human Bromodomains
1085 Recognizes Butyryllysine and Crotonyllysine Histone Peptide
1086 Modifications. *Structure* **2015**, *23*, 1801–1814.
- 1087 (74) Unzue, A.; Zhao, H.; Lolli, G.; Dong, J.; Zhu, J.; Zechner, M.;
1088 Dolbois, A.; Caffisch, A.; Nevado, C. The "Gatekeeper" Residue
1089 Influences the Mode of Binding of Acetyl Indoles to Bromodomains. *J.*
1090 *Med. Chem.* **2016**, *59*, 3087–3097.
- 1091 (75) Madhavi Sastry, G. M.; Adzhigirey, M.; Day, T.; Annabhimoju,
1092 R.; Sherman, W. Protein and Ligand Preparation: Parameters,
1093 Protocols, and Influence on Virtual Screening Enrichments. *J.*
1094 *Comput.-Aided Mol. Des.* **2013**, *27*, 221–234.
- 1095 (76) Wang, R.; Wang, S. How Does Consensus Scoring Work for
1096 Virtual Library Screening? An Idealized Computer Experiment. *J.*
1097 *Chem. Inf. Comput. Sci.* **2001**, *41*, 1422–1426.
- 1098 (77) Ekonomiuk, D.; Su, X. C.; Ozawa, K.; Bodenreider, C.; Lim, S.
1099 P.; Otting, G.; Huang, D.; Caffisch, A. Flaviviral Protease Inhibitors
1100 Identified by Fragment-Based Library Docking into a Structure
Generated by Molecular Dynamics. *J. Med. Chem.* **2009**, *52*, 4860–
4868.
- (78) Bashford, D.; Case, D. A. Generalized Born Models of
Macromolecular Solvation Effects. *Annu. Rev. Phys. Chem.* **2000**, *51*,
129–152.
- (79) Sterling, T.; Irwin, J. J. ZINC 15-Ligand Discovery for Everyone.
J. Chem. Inf. Model. **2015**, *55*, 2324–2337.